JOURNAL OF GEOPHYSICAL RESEARCH, VOL. 104, NO. A6, PAGES 12,515–12,523, JUNE 1, 1999

# Relationships between coronal mass ejection speeds from coronagraph images and interplanetary characteristics of associated interplanetary coronal mass ejections

G. M. Lindsay,[1] J. G. Luhmann,[2] C. T. Russell,[3] and J. T. Gosling[4]

**Abstract.** With an eye toward space weather forecasting and the planned Solar Terrestrial Relations Observatory mission, a combination of Solwind and SMM coronagraph data and Helios-1 and Pioneer Venus Orbiter interplanetary field and plasma data are used to study statistical relationships between the speeds of coronal mass ejections (CMEs) observed near the Sun and key characteristics of the associated interplanetary disturbances (interplanetary coronal mass ejections (ICMEs)) detected near the ecliptic at ≤ 1 AU. When confident associations can be made between the coronagraph observations and interplanetary observations, a predictable relationship is found between observed coronagraph CME speeds and subsequently observed ICME bulk plasma speeds. Consistent with earlier work, the CMEs, regardless of their speed, produce ICMEs moving at least as fast as the minimum solar wind speed. As a rule, the CMEs observed at speeds below the average solar wind speed produce ICMEs that travel faster than the associated CME, implying acceleration, while CMEs with coronagraph speeds above the average solar wind speed produce ICMEs that travel slower than the associated CME, implying deceleration of initially fast low-heliolatitude ejecta. A formula is provided for estimating ICME speed from CME speed. As also previously found, faster CMEs tend to produce ICMEs with larger internal magnetic field magnitudes. While the size and occurrence of southward *Bz* in an ICME are not generally related to the observed CME speed, *Bz* in the sheath region preceding the ICME shows some positive correlation. These observations confirm that while the occurrence of large interplanetary magnetic field magnitudes and high bulk plasma speeds associated with ICME passage may be predictable from coronagraph-derived CME speeds, other important ICME features like large-magnitude southward *Bz* require other diagnostics and tools for forecasts.

## 1. Introduction

In spite of several decades of observations, coronal mass ejection (CME) acceleration and interplanetary propagation (as interplanetary coronal mass ejections (ICMEs,)) remain active areas of research. Important space weather questions yet to be answered include how well CMEs in coronagraph images can be used to predict "geoeffectiveness" during future missions such as NASA's Solar Terrestrial Relations Observatory (STEREO) mission. The STEREO mission concept places a solar coronagraph at a large angle from the Earth-Sun line to observe Earth-bound CMEs. While it is known that ICMEs moving faster than the solar wind speed produce preceding shocks, compressed solar wind, and interplanetary magnetic field (IMF), and generally larger interplanetary disturbances [e.g., *Tsurutani et al.*, 1990; *Gosling et al.*, 1991; *Gonzalez et al.*, 1994, and references therein], debate continues on the relationships between solar CME observations and ICMEs and on the importance to ultimate geomagnetic response of interplanetary propagation-related changes. *Hirshberg et al.* [1974], *Burlaga et al.* [1987], and *Gosling et al.* [1987a] recognized that the solar wind stream structure could alter an ICME in transit by adding to its compression and reorienting both the internal and surrounding flows and fields. *Gosling and McComas* [1987] illustrated how the orientation of the ambient IMF in particular could enhance an ICME's geomagnetic effectiveness by adding large southward components (*-Bz*) in the solar wind pileup or sheath region preceding a fast ICME. *Gonzalez et al.* [1998] recently showed that in addition, faster ICMEs generally have higher internal magnetic field magnitudes. Because ICME fields are often at large inclinations (e.g., as in clouds or interplanetary flux ropes) [*Klein and Burlaga*, 1982], larger field magnitudes generally mean larger *Bz* components. Given this complicated collection of influences, it is reasonable to ask if one can expect to gain useful information on ICMEs from coronagraph images of CMEs obtained at large-angle perspectives as is planned for STEREO. The present study uses combinations of Solwind and Solar Maximum Mission (SMM) coronagraph observations and Helios-1 and Pioneer Venus Orbiter (PVO) interplanetary data to illustrate how well key ICME characteristics, such as velocity, magnetic field magnitude (internal and piled up ambient field), and the north-south magnetic field component *Bz* statistically relate to coronagraph observations of CME velocity. It thereby provides a test of the large-angle (here called quadrature) coronagraph approach and adds some insights on the associations between coronagraph CMEs and ICMEs.

[1]Space-Based Warning Branch, Headquarters, Air Force Space Command, Peterson Air Force Base, Colorado Springs, Colorado.
[2]Space Sciences Laboratory, University of California, Berkeley.
[3]Institute of Geophysics and Planetary Physics, University of California, Los Angeles.
[4]Los Alamos National Laboratory, Los Alamos, New Mexico.



Paper number 1999JA900051.
0148-0227/99/1999JA900051$09.00

Quadrature situations provide a unique way of comparing the characteristics of CMEs and ICMEs because the coronagraph images give an effective cross-sectional view of what is headed toward the spacecraft. The quadrature configurations used here were possible because Earth-orbiting coronagraphs were observing the Sun at the same time that an interplanetary spacecraft was located above the Sun's limb. *Burlaga et al.* [1982] describe an early application of the quadrature technique, which was followed by several other studies by *Schwenn* [1983], *Sheeley et al.* [1985], and *Richardson et al.* [1994], who compared coronagraph CMEs with detections of interplanetary shocks. In the studies of both Sheeley et al. and Schwenn the characteristics of the ICMEs driving the shocks in interplanetary space were not specifically examined, although a few examples were shown. In the work of Richardson et al. the ICMEs were examined; however, the focus of their study was the interplanetary shocks and their location with respect to the expected solar source of the ICME, rather than the characteristics of the resulting interplanetary disturbance.

Associations between ICME signatures such as interplanetary shocks observed by spacecraft near the Earth and solar observations are often ambiguous because the apparent sources in the corona are inferred from secondary signatures such as disappearing filaments, two-ribbon flares, type II and IV radio bursts, or long-duration X-ray events [*Feynman and Martin*, 1995; *Richardson et al.*, 1994; *Kahler*, 1993; *Mihalov*, 1985; *Cane*, 1985; *Munro et al.*, 1979]. While these signatures are often related to CME occurrence, the connection between their characteristics and the characteristics of the actual CMEs is not known. Moreover, the shock has its own speed and may extend far beyond the ejecta driving it. As a consequence, comparing characteristics such as speed in the corona and in interplanetary space is not as straightforward as it is in quadrature cases of pairs of CMEs and ICMEs.

Coronagraph-derived CME speeds and their implications for ICMEs have been previously studied by a number of authors [e.g., *Gosling et al.*, 1976; *Howard et al.*, 1985; *Hundhausen et al.*, 1994]. Within the Skylab and SMM coronagraph 2-10 solar radii ($R_s$) field-of-view limits, it was found that CMEs exhibited speeds in the range ~35 to ~2000 km/s. *Hundhausen et al.* [1994], taking into account line-of-sight issues inherent in coronagraph determinations of speed, concluded that the slowest CMEs are accelerated beyond the SMM maximum field of view of 4-6 $R_s$ as interplanetary bulk plasma speeds below ~290 km/s are rare. Hundhausen et al. also showed that some higher speed CMEs appeared to be accelerating as they left the SMM coronagraph field of view while others had a constant speed profile. From a combination of Solwind coronagraph observations and Helios-1 interplanetary observations, *Sheeley et al.* [1985] found that some CMEs observed traveling in the corona below the average solar wind speed (~200-300 km/s) could be linked to ICME-related interplanetary shocks at Helios-1's heliocentric distances of 0.3-1.0 AU. These observations implied that slow CMEs can be accelerated in the high corona or inner heliosphere to speeds higher than the ambient solar wind speed or may produce ICMEs expanding at supermagnetosonic speeds. *Gosling et al.* [1976] and *Sheeley et al.* [1985] showed that in contrast, some CMEs observed traveling at high speeds appear to produce slower ICMEs. Recent Solar and Heliospheric Observatory (SOHO) Large Angle Spectrometric Coronagraph (LASCO) observations, which extend the coronal speed versus altitude measurements to ~30 $R_s$ [e.g., *Sheeley et al.*, 1997], provide a better idea of the altitude at which some CMEs reach their asymptotic speeds. Nevertheless, some are still accelerating as they cease to be trackable, and the much more detailed measurements from this multirange coronagraph confirm the SMM result of *Hundhausen et al.* [1994] that the speed also depends on the CME feature that is tracked. While the general issue of CME acceleration clearly merits further study, here we focus on the extent to which characteristics of ICMEs can be inferred from CME speeds using quadrature configurations. Because quadrature opportunities with well-placed interplanetary spacecraft are limited for LASCO, we use earlier coronagraph measurements catalogued for Solwind and SMM coronagraphs by *Sheeley et al.* [1980, 1985, also personal communication, 1994] and *Burkepile and St. Cyr* [1993], respectively. As mentioned above, PVO and Helios-1 provide the ICME information. The resulting statistical relationships between CME and ICME speeds and between CME speed and ICME-associated IMF perturbations, two items of primary interest in space weather forecasting, indicate the extent to which CME speeds in the corona can be used to predict ICME characteristics in interplanetary space.

## 2. Data Sources

Solwind was launched on February 24, 1979, into a nearly circular orbit ~500 km above the Earth's surface and inclined 97° to the equator. The orbit was in the noon-midnight meridian, and the orbital period is 97 min. Briefly, the Solwind coronagraph observed a 2.6-10 ($R_s$) annular field of view with a spatial resolution of 1'25" (refer to *Koomen et al.* [1975] for more detail). Full-field coronal images were obtained at 10-min intervals (and occasionally at 5-min intervals) during the ~1 hour sunlit portion of each orbit. This mode of operation continued without interruption from the time of instrument turn on March 28, 1979 to June 19, 1979. From June 19, 1979, the coverage is less complete, with the spacecraft configured for solar observation only 60% of the time. Observations were made until the end of September 1985. A full catalogue of the CME observations from the Solwind coronagraph was provided by N. Sheeley (personal communication, 1994). His list gives the date and time of ejection, height, speed, and angular position of the CME center. Comments are also included describing the CME morphology and other associated solar activity.

The Solar Maximum Mission (SMM) observatory was launched February 14, 1980, into a 574 km altitude circular orbit inclined 28.5° to the equator. The ~95-min period of each SMM orbit was divided into roughly 60 min of satellite day and 35 min of satellite night. A detailed description of the SMM coronagraph-polarimeter instrument is found in the work of *MacQueen et al.* [1980]. This instrument obtained data from March through September in 1980 and then in 1984-1989. An electronics failure rendered it inoperative in the interim. The telescope produced an image of the corona with a square field of view extending from 1.6 to 4.1 $R_s$ at the sides and out to just over 6.0 $R_s$ along the diagonals. Images were frequently taken at high spatial resolution of 6" in March 1980 and immediately following the repair in 1984. However, the normal mode of observation produced coronagraph images in low-resolution mode, wherein the spatial resolution was 12". The CMEs observed by the SMM coronagraph have been catalogued by *Burkepile and St. Cyr* [1993].

One source of interplanetary data used in this study is the Pioneer Venus Orbiter (PVO) spacecraft from which full plasma and magnetic field measurements were available from 1979 to 1988. This is approximately the duration of solar cycle 21. PVO was launched May 29, 1978, and entered Venus orbit on December 4, 1978, and the deep Venus atmosphere in late 1992. The spacecraft, its mission, and its instrument complement are described by *Colin* [1980]. The primary instruments providing the interplanetary measurements were the magnetometer [*Russell et al.*, 1980] and the plasma analyzer [*Intriligator et al.*, 1980].

For our purpose, the average 10-min resolution University of California, Los Angeles (UCLA) magnetometer data and the full 9-min resolution plasma data as derived by the Ames Research Center investigators (both archived at the National Space Science Data Center (NSSDC)) were used.

Helios-1 provided the second source of interplanetary data used in this study. Helios-1 was launched in December 1974 and injected into a Sun centered orbit with a perihelion of ~0.3 AU and an aphelion of ~1 AU. Helios-1 spends half of its orbit above the solar equator and half of its orbit below the solar equator. Helios-1 frequently dwelt for ~5 months within 30° of the east or west solar limb as viewed from Earth, making it quite useful for quadrature studies. A biaxial magnetometer [*Mariani et al.*, 1978] provided measurement of the IMF (three components and magnitude). The solar plasma characteristics were measured by the plasma analyzer from the Max-Planck-Institut für Physik und Astrophysik at Garching and the Max-Plank-Institut für Aeronomie at Lindau, Federal Republic of Germany [*Schwenn*, 1983]. The instruments on Helios-1 returned reliable data until December 1982.

## 3. Data Analysis

Helios-1 and PVO both provided a quadrature configuration for extensive periods of time. The quadrature configuration in our study occurs when one of these interplanetary spacecraft is near the solar limbs as viewed from Earth (~90° with respect to the Earth-Sun line; see Figure 1). The orbital positions and relevant dates of Helios-1 and PVO coverage are shown in Figures 1 and 2. Figure 1 shows the Helios-1 orbit in a fixed Sun-Earth system during 1979-1982. Reference lines are drawn at 32° relative to the east-west directions. Figure 2, also in a fixed Sun-Earth system, shows the orbital positions of PVO during quadrature periods from 1979 to 1988 when data were available. Different symbols are used to show the start and stop points of the interval of data examined. During 1979-1988, PVO was within +30° of the Sun's east or west limbs 12 times, often for periods lasting nearly 4 months. During 1979-1981, Helios-1 spent ~85% of the time within ±30° of the Sun's limbs [*Schwenn*, 1983]. The

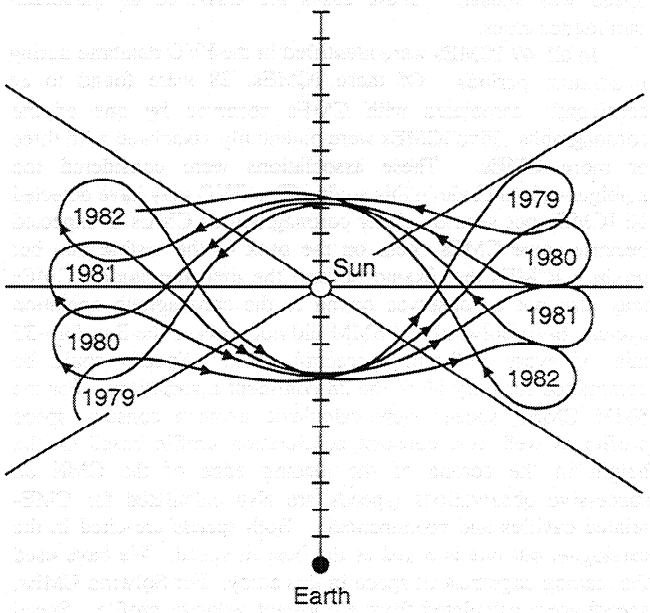


**Figure 1.** The Helios-1 orbit in a fixed Sun-Earth system during 1979-1982. Reference lines are drawn at 32° relative to the east-west directions.

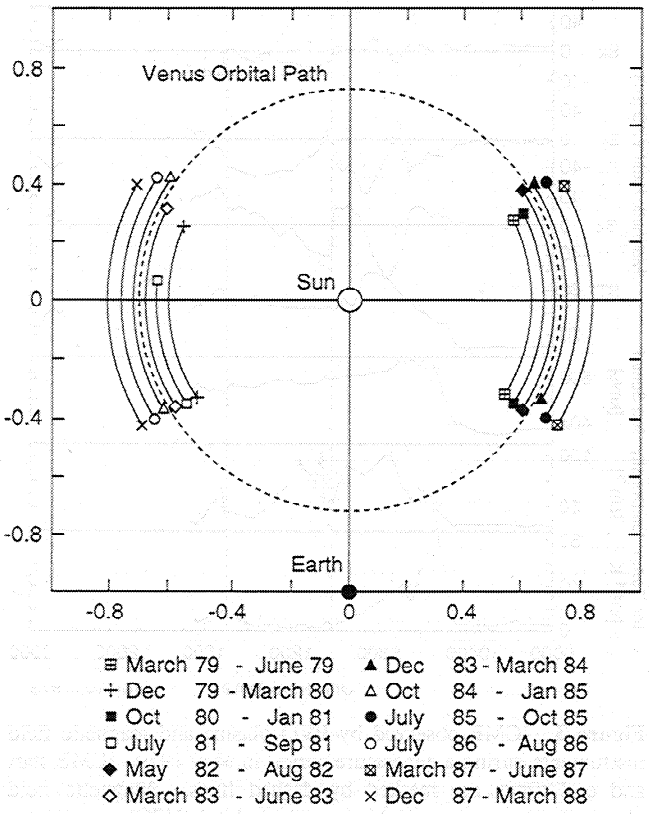


**Figure 2.** Locations of Polar Venus Orbiter (PVO) with respect to the Earth during quadrature periods.

interplanetary plasma and field data from the PVO and Helios spacecraft overlapped with the solar observations provided by the Solwind (1978-1984) and SMM (1980 and 1984-1989) coronagraphs.

ICMEs observed in interplanetary space by plasma spectrometers and magnetometers typically exhibit a combination of features: a decrease in ion temperature below ambient, a monotonically decreasing ion speed, and an elevated ion dynamic pressure and density, combined with a significant rotation of the magnetic field over about a day [e.g., *Lindsay et al.*, 1994]. In the present study, all these signatures were required to classify a structure observed in the solar wind as an ICME. A similar identification scheme was originally used by *Burlaga et al.* [1981] with the additional requirement of higher than ambient fields. However, *Gosling et al.* [1987b] showed examples in which the high field signature required by Burlaga et al. was not observed. Field magnitude was therefore not used as a criterion for identifying interplanetary CMEs in this study. In the PVO database used here, ICMEs (identified in the manner stated above) have an occurrence rate that is in phase with the solar cycle [*Lindsay et al.*, 1994]. This is consistent with the variation in occurrence rate found by *Gosling et al.* [1992] using counterstreaming suprathermal solar wind electrons to identify ICMEs at 1 AU and by *Webb* [1991] using CMEs identified in the SMM coronagraph images. Most of the interplanetary shocks identified in the PVO database are found to be driven by plasma and fields exhibiting the characteristics prescribed to ICMEs, further reinforcing our identification scheme.

Figure 3 shows an ICME detected by the PVO spacecraft at 0.7 AU on May 10, 1979. The top three traces display the components of the interplanetary magnetic field (IMF) in Venus Solar Orbital (VSO) coordinates. In this coordinate system, $x$ is directed radially from Venus to the Sun, $y$ lies in the Venus

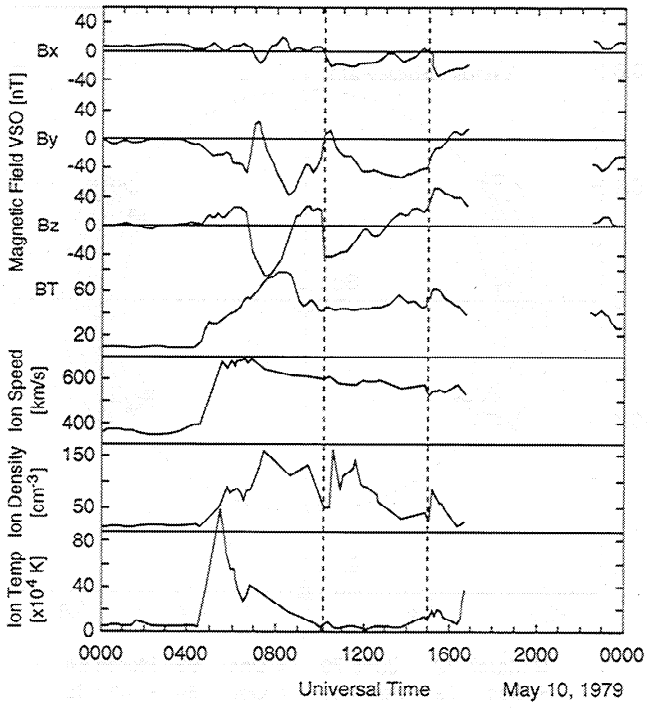


**Figure 3.** ICME observed by PVO plasma and magnetic field instruments during a quadrature period in May 1979. ICME start and end times are marked by dashed lines. Magnetic field observations are given in Venus solar orbital (VSO) coordinates with the x direction toward the sun and the z direction along the orbital pole.

orbital plane and is positive in the direction opposite planetary motion, and $z$ completes the right-hand system, pointing north out of the Venus orbital plane. The IMF magnitude ($Bt$), ion bulk speed, ion density, and ion temperature are shown in the bottom four traces. In this paper, the term ICME is reserved for what is considered the actual coronal ejecta in interplanetary space, not including the disturbed solar wind preceding it, which is referred to as sheath. The ICME leading and trailing edges (noted by the dashed lines) indicate that at 0.7 AU it is ~0.1 AU (~20 $R_s$) in length along the spacecraft trajectory. It is traveling at a bulk speed (the average speed of the measured portion of the ICME) of ~600 km/s and is driving an interplanetary shock observed on PVO at 0430 UT on May 10, 1979. Compression of the ambient field ahead of the ICME in the sheath region creates IMF magnitudes that are much larger than ambient (~70 nT compared with ~12 nT), while draping and compression produce large southward fields (~50 nT). The ICME is also characterized by large IMF magnitudes (~50 nT) and a southward field (~35 nT).

Identification of the CME in coronagraph data that are associated with an observed ICME is done by timing and location. In the corona the ejecta must be accelerated from rest by a combination of thermal and magnetic forces [e.g., *Low*, 1990]. At the point at which the action of these forces ceases, the ejecta that subsequently appear as ICMEs will have reached maximum speed. Beyond this point the ejecta will either be carried out with the solar wind at the solar wind speed (if the ejecta have merely been accelerated to the minimum speed) or will decelerate if they interact with the slower solar wind ahead. Previous reports suggest that the typical region of acceleration appears to lie within tens of solar radii. The ejecta are expected to travel at a constant speed or decelerate for most of their interplanetary flight. The time of ejection from the Sun is often estimated from the bulk speed of an ICME, assuming constant speed and radial propagation. However, if the ejecta decelerate in transit, the inferred ejection time will be earlier than that estimated.

The case shown in Figures 3 and 4 illustrates the association technique used here. The ~600 km/s ICME bulk speed seen in Figure 3 implies an average time of travel between the Sun and PVO of 50 hours. The estimated ejection time is then ~0900 UT on May 8, 1979. The coronagraph databases are searched for a CME observed on the appropriate limb of the Sun near the time predicted from the ICME bulk speed. Since it is not known whether deceleration or acceleration has occurred since leaving the coronagraph field of view, a window of 12 hours centered on the predicted ejection time is searched. A CME occurring in coronagraph observations during this window is considered to be a candidate match. Solwind observed only one CME (shown in Figure 4) occurring on the west limb of the Sun within 12 hours of the estimated time of ejection for the ICME shown in Figure 3. The time of the CME is May 8, 1979, at 1028 UT slightly later than that estimated. When the CME left the coronagraph field of view (~10 Rs), it had a speed of ~500 km/s. At 0.7 AU the apparently associated ICME had a bulk speed of ~600 km/s, suggesting that ejecta must have been accelerated between the corona and 0.7 AU. The fact that the CME had a loop like structure and very high density in the corona [*Sheeley et al.*, 1980] and that the associated ICME had a flux rope type structure and a density much higher than ambient strengthens our confidence in this association.

The event-pairing techniques used here resulted in 12 ICMEs observed by PVO reasonably associated with only one possible coronagraph CME. These cases are classified as high-confidence cases. That only a single CME was found at the appropriate limb in the estimated time window lends credence to the associations made. Additionally, in 11 of the 12 high-confidence cases the preceding and following ICMEs observed by PVO occurred at least 36 hours prior to or following the ICME associated with a coronagraph CME. To avoid any ambiguity due to the proximity of ICMEs, we used only these 11 events. Eight of the ICMEs observed by PVO were each associated with two possible coronal CMEs. In these cases, the CME occurring at the time closest to the time predicted from the ICME bulk speed was chosen. These cases are classified as moderate-confidence cases.

In all, 49 ICMEs were identified in the PVO database during quadrature periods. Of these ICMEs, 28 were found to be confidently associated with CMEs observed by one of the coronagraphs. Five ICMEs were potentially associated with three or more CMEs. These associations were considered too ambiguous to include in this study. That PVO may have detected 16 ICMEs not seen by either coronagraph as CMEs is expected because some CMEs occur on the back of the visible Sun but produce ICMEs that extend beyond the limb longitude. CMEs may also not be observed owing to the coronagraph operation cycles. Both Solwind and SMM did not observe the Sun for ~35 min of every ~90-min spacecraft orbit. Speeds could be determined for only 19 of the 28 confident associations. For the SMM CMEs, speeds were calculated using a constant speed profile as well as a constant acceleration profile based on the height in the corona of the leading edge of the CME on successive observations (speeds are also calculated for CME-related cavities and prominences). Both speeds are cited in the catalogue, but one is noted as the best fit speed. We have used the leading edge best fit speed in this study. For Solwind CMEs, speeds were calculated from a constant velocity profile. Speed was determined only if the feature was distinct enough to measure against the background corona and to be seen on successive images [*Hundhausen et al.*, 1994].

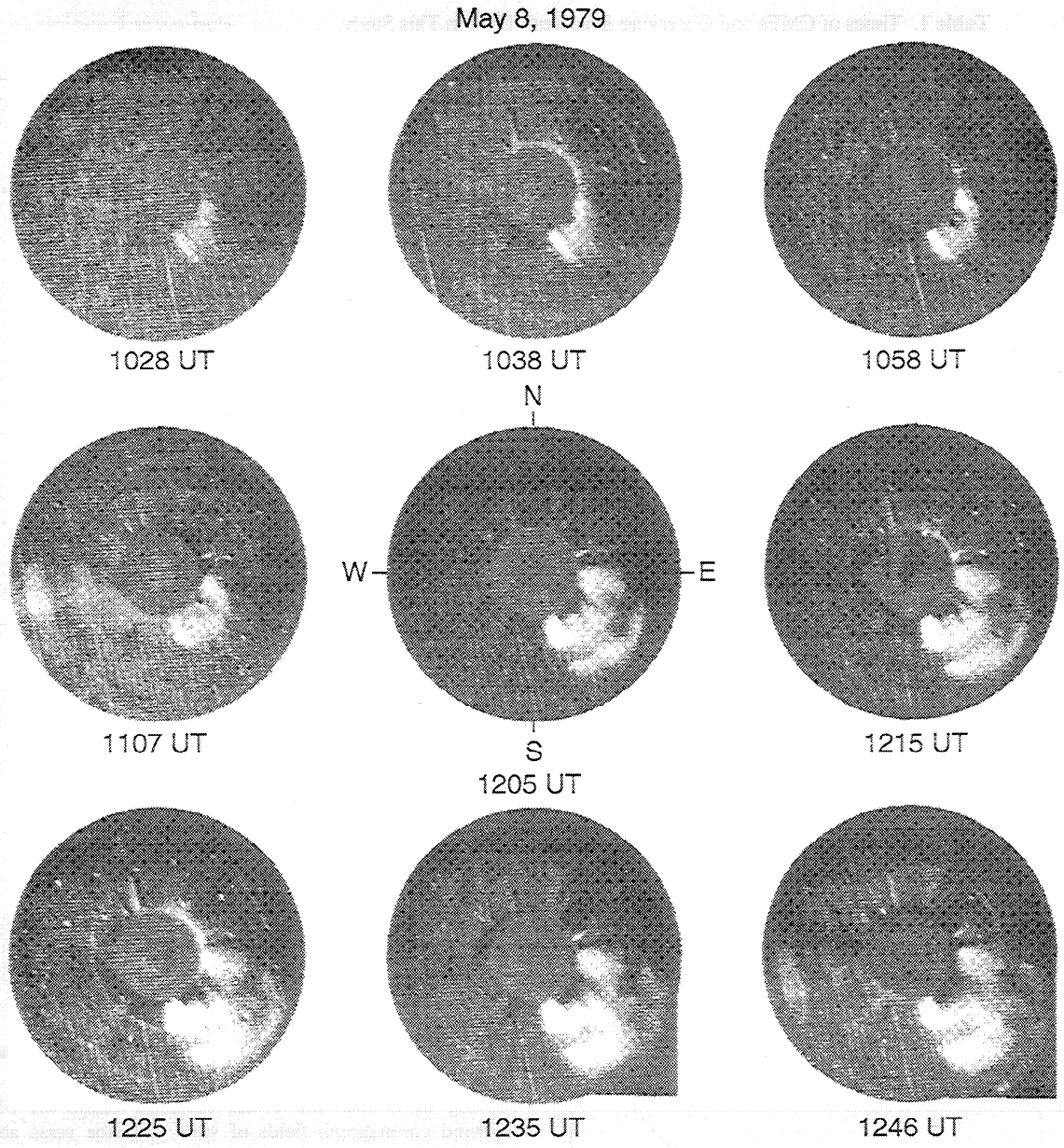


**Figure 4.** CME observed by Solwind coronagraph that is associated with the ICME shown in Figure 3.

The Helios-1 interplanetary ICMEs used in this study are extracted from the analysis of *Sheeley et al.* [1985]. Sheeley et al. identified 56 interplanetary shocks observed in 1979-1982 by the Helios spacecraft when it was in quadrature with the Solwind coronagraph. Additionally, an ICME event detected by Helios-1 on May 14, 1982, and cited by *Schwenn* [1983] is included. Here the Helios plasma and field data were used in the same manner as the PVO data, with the ICME body speeds distinguished from the shock speeds. (Not all of Sheeley et al.'s, cases had clear driver signatures. Hence we used a subset of their cases.) The complete data set used in this study thus consists of 19 ICMEs observed by PVO and 12 observed by Helios-1. Table 1 lists the observing spacecraft and the date that an ICME's leading edge is observed along with the coronagraph and the date of the observation of the associated CME in the corona. The confidence rating is also noted for each case. Of the 19 PVO ICMEs, 4 were associated with CMEs observed by SMM and 15 were associated with CMEs observed by Solwind. All 12 Helios ICMEs were associated with CMEs observed by Solwind. One ICME, associated with the May 8, 1979, Solwind observations shown in Figure 4, was detected by PVO at 0.7 AU and then by Helios-1 at 0.98 AU. This event has also been described in papers by *Michels et al.* [1980] and *Burlaga* [1991].

## 4. Results

Plotted in Figure 5 is the bulk speed (the average speed of the structure) of the ICMEs observed in interplanetary space between 0.7 and 1.0 AU versus the speed of the associated CMEs observed in the corona. The dashed line shows where the observed interplanetary speed equals the observed speed in the corona. Open circles represent those cases where only one coronagraph CME occurred near the estimated time of ejection predicted from the observed ICME bulk speed (high-confidence cases). Solid circles represent those cases where two or three possible coronagraph CMEs occurred near the predicted time of ejection. For these cases, only the one closest to the predicted

**Table 1.** Times of CMEs and Observing Spacecraft Used in This Study.

| | Interplanetary CME | | | Coronal CME | | | |
|---|---|---|---|---|---|---|---|
| Case | Date | Time, UT | Spacecraft | Date | Time, UT | Coronagraph | Confidence |
| 1 | May 10, 1979 | 1000 | PVO | May 8, 1979 | 1028 | Solwind | moderate |
| 2 | May 28, 1979 | 2230 | Helios-1 | May 27, 1979 | 1044 | Solwind | moderate |
| 3 | July, 5, 1979 | 1500 | Helios-1 | July 3, 1979 | 0156 | Solwind | high |
| 4 | July 21, 1979 | 1700 | PVO | July 19, 1979 | 1010 | Solwind | high |
| 5 | March 17, 1980 | 0900 | PVO | March 13, 1980 | 0955 | Solwind | high |
| 6 | March 19, 1980 | 0200 | PVO | March 16, 1980 | 0957 | Solwind | high |
| 7 | March 22, 1980 | 1400 | Hilios-1 | March 19, 1980 | 0706 | Solwind | high |
| 8 | March 30, 1980 | 0400 | Helios-1 | March 27, 1980 | 1358 | Solwind | high |
| 9 | May 23, 1980 | 0200 | Helios-1 | May 21, 1980 | 2143 | Solwind | high |
| 10 | June 20, 1980 | 0600 | Helios-1 | June 18, 1980 | 0757 | Solwind | high |
| 11 | June 23, 1980 | 1300 | Helios-1 | June 20, 1980 | 1530 | Solwind | high |
| 12 | July 11, 1980 | 1830 | Helios-1 | July 9, 1980 | 0158 | Solwind | high |
| 13 | July 21, 1980 | 1500 | Helios-1 | July 18, 1980 | 0842 | Solwind | high |
| 14 | Aug. 1, 1980 | 1600 | Helios-1 | July 29, 1980 | 1331 | Solwind | moderate |
| 15 | Nov. 15, 1980 | 0200 | Helios-1 | Nov. 14, 1980 | 0820 | Solwind | moderate |
| 16 | May 14, 1981 | 1200 | Helios-1 | May 13, 1981 | 0415 | Solwind | high |
| 17 | July 6, 1981 | 0600 | PVO | July 4, 1981 | 1506 | Solwind | moderate |
| 18 | Aug. 23, 1981 | 0600 | PVO | Aug. 19, 1981 | 1346 | Solwind | moderare |
| 19 | Sept. 17, 1981 | 2200 | PVO | Sept. 15, 1981 | 0916 | Solwind | moderate |
| 20 | Oct. 9, 1981 | 0100 | PVO | Oct. 7, 1981 | 0303 | Solwind | high |
| 21 | Oct. 13, 1981 | 2000 | PVO | Oct. 12, 1981 | 0533 | Solwind | high |
| 22 | Oct. 28, 1981 | 2000 | PVO | Oct. 24, 1981 | 0132 | Solwind | high |
| 23 | Aug. 18, 1982 | 0600 | PVO | Aug. 14, 1982 | 0214 | Solwind | high |
| 24 | May 2, 1983 | 1100 | PVO | April 28, 1983 | 0624 | Solwind | high |
| 25 | Jan. 24, 1984 | 1000 | PVO | Jan. 22, 1984 | 0841 | Solwind | moderate |
| 26 | Jan. 26, 1984 | 1200 | PVO | Jan. 23, 1984 | 0210 | Solwind | moderate |
| 27 | Feb. 17, 1984 | 1300 | PVO | Feb. 15, 1984 | 1917 | Solwind | high |
| 28 | July 17, 1986 | 0100 | PVO | July 14, 1986 | 0237 | SMM | high |
| 29 | Aug. 12, 1986 | 1600 | PVO | Aug. 6, 1986 | 1952 | SMM | moderate |
| 30 | March 23, 1988 | 2300 | PVO | March 20, 1988 | 2100 | SMM | high |
| 31 | March 29, 1988 | 2000 | PVO | March 26, 1988 | 2306 | SMM | moderate |

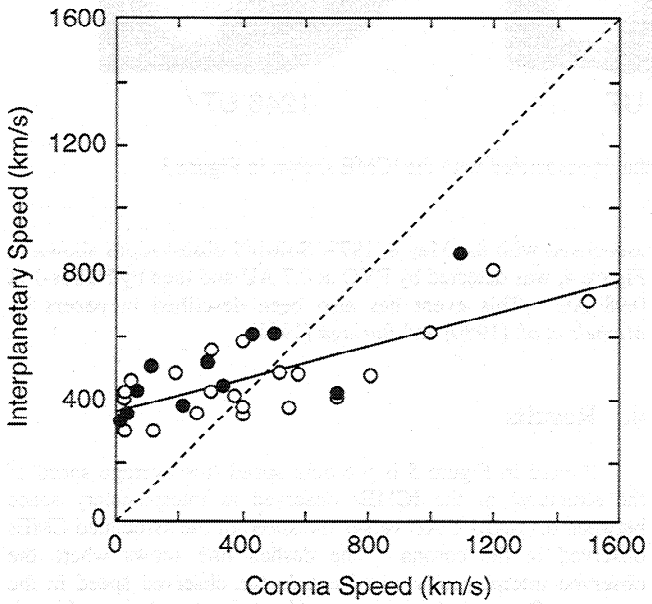


**Figure 5.** Speed of ICME plotted as a function of the associated CME speed in the corona. Open circles represent high confidence cases. Solid circles represent moderate-confidence cases. The formula describing the line fitted to the data is $V_{IP} = (0.25 \pm 0.04)\ V_c + 360 \pm 23$.

time is plotted (moderate confidence). This display shows that below 500 km/s most of the CMEs produce ICMEs that are moving faster than the CMEs observed within the SMM and Solwind coronagraph fields of view and vice versa above 500 km/s. There also appears to be a minimum speed of ~330 km/s attained by all ICMEs that is comparable to the slowest speeds of the solar wind and below the ~380-420 km/s average speed of the solar wind. Thus regardless of what speed is observed in the limited field of view of the coronagraph, all CMEs are associated with ICMEs moving at least at the slow solar wind speed consistent with what *Gosling et al.* [1987b, 1994] found from analyses of ICMEs observed in and out of the ecliptic plane. The faster group of CMEs (> ~500 km/s) are, in contrast, associated with ICMEs moving at speeds lower than their coronal counterparts, implying deceleration of ejecta in transit, at least at low heliolatitudes. The solid line in Figure 5, whose formula is given in the caption, represents a simple linear fit to the data shown. Separate line fits for the high, and moderate-confidence cases yield similar results. Even though the individual ICMEs are not necessarily decelerating or accelerating in a uniform manner and are detected at a range of heliocentric distances (0.7-1.0 AU), a straight line gives a good description of the relationship between the CME and ICME speeds.

The maximum IMF magnitudes occurring in the ICMEs are shown in Figure 6a as a function of the speeds of the associated CMEs in the corona. Ten of the cases in Figure 5 could not be used here owing to gaps within the ICME data that made

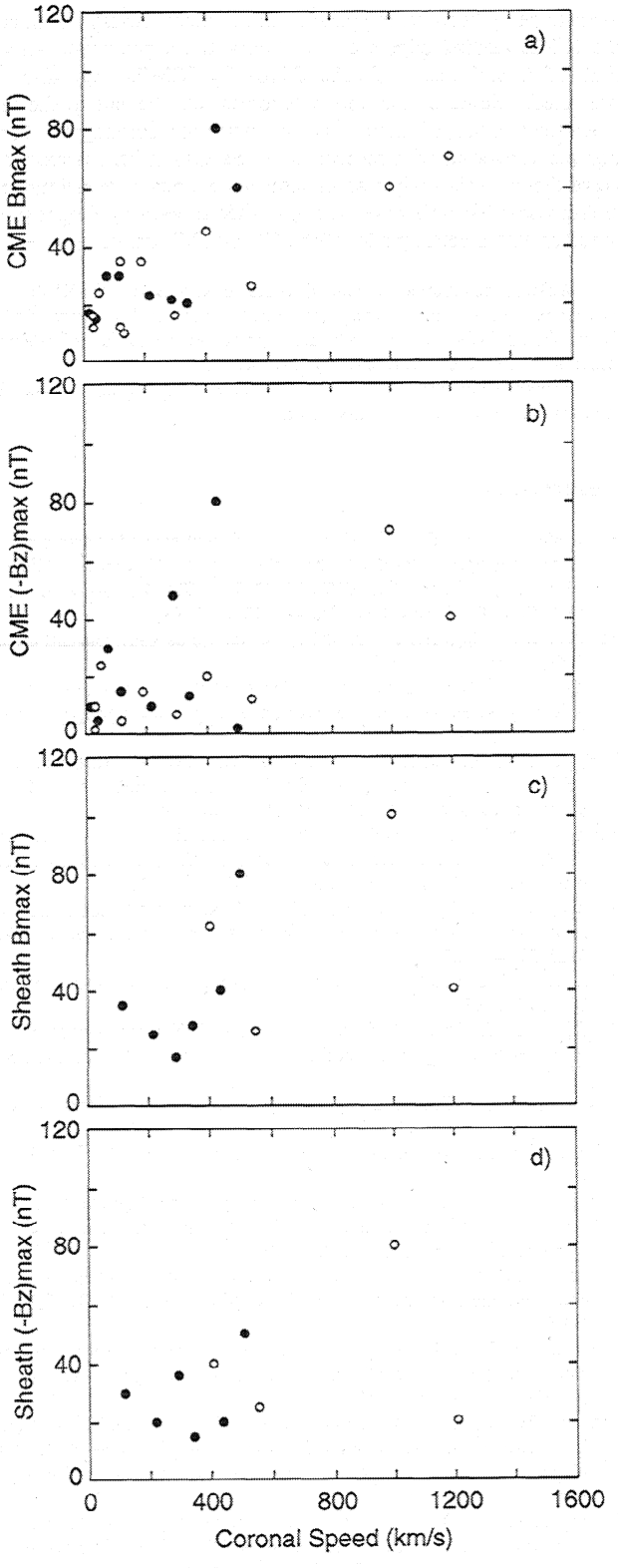


**Figure 6.** (a) Maximum field magnitude within ICMEs as a function of the associated CME speed in the corona. (b) Maximum southward field magnitude in ICMEs as a function of the associated CME speeds. (c) Maximum field magnitude in ICME sheath in interplanetary space plotted as a function of the associated CME speed. (d) Maximum southward field magnitude in ICME sheath plotted as a function of the associated CME speed for the cases in Figure 6c. In Figure 6c only ICMEs with preceding shocks are included. Symbols are the same as in those in Figure 5.

determining the maximum IMF strength impossible. Although there is considerable scatter, the CMEs with higher speeds on average foretell larger maximum IMF magnitudes in their associated ICMEs. It is not clear whether this trend is due to an initially larger CME field in the corona [e.g., see *Gonzalez et al.*, 1998] or is a result of the interaction between the ICME and the ambient solar wind ahead, or both. In most of these cases the maximum IMF magnitude occurs in the leading portion of the ICME, suggesting that the compression of the ICME leading edge is an important effect. Recently, *Farrugia et al.* [1995] suggested that strong IMF magnitudes may occur within the CME, near the leading edge, as a result of expansion, because the spacecraft samples younger, stronger fields first and older, weaker fields at the trailing edge. However, this effect would not produce the observed relationship between CME speed and ICME field strength.

Figure 6b shows the maximum southward component of the IMF occurring in ICMEs versus the speed of the associated CMEs in the corona. As in Figure 6a, 12 cases could not be used in Figure 6b owing to gaps in the ICME data. Of the 21 remaining CMEs, the 2 exhibiting the largest speeds in the corona also have the largest southward fields in the associated ICMEs detected at 0.7 AU. However, the bulk of the points show no regular trend in the size of southward $Bz$ as a function of CME speed in the corona. This result is reasonable because ICMEs can have any orientation with respect to the Venus or Helios-1 orbital plane. Thus their internal magnetic fields may also have any orientation, producing a variety of observed southward $Bz$ magnitudes.

Figure 6c shows the maximum IMF magnitude occurring in the sheath region between the ICME and its leading interplanetary shock versus the speed of the associated CME in the corona. Only 10 of the 23 PVO ICMEs examined in Figures 5 and 6 were driving interplanetary shocks, but this set predictably includes all ICMEs with associated CME speeds greater than the average solar wind speed of ~375 km/s. One case (May 10, 1988, shown in Figure 3) has data gaps in the sheath region that make the determination of the maximum IMF magnitude impossible. For the remaining nine cases, Figure 6c shows a trend toward higher IMF magnitudes for higher speeds in the corona. One might expect that the faster an ICME travels, the more it compresses the ambient solar wind ahead and therefore the more likely it is to be associated with larger sheath fields. Figure 6c also shows that four ICMEs driving interplanetary shocks have associated CME speeds less than the average solar wind speed. *Gosling et al.* [1991] noted that ICMEs traveling near the average solar wind speed did not usually produce geomagnetic storms. However, these slow ICMEs are both accompanied by interplanetary shocks and produce sheath IMF magnitudes much larger than ambient (~28-80 nT). Thus even slow CMEs may precede ICMEs with geoeffective traits that can produce storms, though not usually the largest storms.

Figure 6d shows the maximum southward component of the IMF occurring in the sheath region between the ICME and its interplanetary shock versus the speed of the associated CME. Again, 14 cases shown in Figures 5 and 6 are not included here, because the ICMEs were not driving interplanetary shocks or significant data gaps were present. The few data points shown suggest that larger southward $Bz$ occurs in the sheath region for coronagraph CMEs with higher speeds but that the correlation is not high. This result can be understood because although compression and draping in the sheath region result in a higher likelihood of large $Bz$ [*Gosling and McComas*, 1987], the sign and magnitude of the sheath $Bz$ depend on both the IMF and ICME orientation. Thus high CME speed may be regarded as a necessary but insufficient condition for high sheath southward fields.

## 5. Conclusions

By comparing a number of CMEs observed by coronagraphs with their counterparts (ICMEs) observed in interplanetary space, this study observationally confirms that CMEs that are slow (less than the slowest solar wind speeds) in the corona are associated with ICME speeds of at least the slow solar wind speed as was previously inferred by *Gosling et al.* [1991, 1994] and *Hundhausen* [1994]. CMEs that are fast in the corona are associated with fast ICMEs, although the ICMEs are usually moving slower than the CMEs. For the faster CMEs there is a trend toward larger IMF magnitudes within the associated ICMEs, but no clear trend exists for the magnitude of southward *Bz*. To predict the direction of the fields within the ICME, a greater understanding of the orientation of the ICME with respect to the Sun's magnetic field configuration is required [e.g., *Hoeksema and Zhao*, 1992]. When ICMEs are preceded by interplanetary shocks, the magnitudes of both the total field and the southward field in the sheath region show some increase with increasing CME speed, but the latter correlation is less consistent. While the fast CMEs are generally associated with ICMEs with leading shocks, slow CMEs are also occasionally associated with ICME shocks.

As in the study of *Sheeley et al.* [1985], we find that CMEs with speeds greater than ~500 km/s pair with slower ICMEs, suggesting deceleration of ejecta as they travel outward in the low-latitude heliosphere. CMEs with speeds less than the average solar wind speed pair with faster ICMEs, implying acceleration between the corona and the location of the ICME. Acceleration is sometimes observed to occur throughout the LASCO field of view to ~30 $R_s$ [*Sheeley et al.*, 1997]. The slow CMEs in this study may often accelerate beyond the limited fields of view of the SMM and Solwind coronagraphs. Moreover, their speeds in the corona may depend on whether they are flare or prominence associated. *Gosling et al.* [1976] and *Feynman and Martin* [1995] concluded that within a 1.75-6 $R_s$ field of view, flare-associated events travel faster than events associated with eruptive prominences. This implies that CMEs associated with flares are likely to reach their maximum speed within the SMM or Solwind field of view. CMEs associated with eruptive prominences may still be accelerating as they leave the coronagraph field of view. Indeed, *Gosling et al.* [1980], *Marubashi* [1986], *Burlaga* [1988], and *Tang et al.* [1989] identified ICMEs associated with eruptive prominences that were driving interplanetary shocks at ~1 AU.

Theories are being formed and MHD models developed describing the formation, ejection, and transit of CMEs through the corona and the heliosphere [e.g., *Low*, 1990; *Chen and Garren*, 1993; *Cargill et al.*, 1995]. The relationship between the speed of a CME in the corona and the subsequent ICME speed found here can be used as a baseline for comparison with the behavior predicted by the models. In addition, the trends observed in the variation of the field magnitudes should be replicated by any realistic model. Detailed IMF *Bz* predictions require much more sophisticated approaches than those used by most of these current models.

With a coronagraph positioned ~90° from the Earth-Sun line, it is possible to forecast an arrival time window of an ICME and its expected speed at 1 AU using the relationship to CME speed shown in Figure 5. While the arrival time estimate is compromised by a lack of knowledge of the acceleration or deceleration profile, at least limits can be set using the CME speed and a predicted ICME speed from Figure 5. However, the observed CME speed does not enable the prediction of whether the ICME will drive an interplanetary shock, unless the CME has a speed in the corona greater than the average solar wind speed of ~375 km/s. Using the result from *Gosling et al.* [1987b] that the average delay between the passage of an interplanetary shock and the ICME leading edge was ~13 hours, the approximate arrival time of interplanetary shocks driven by ICMEs may also be predicted. Some of the above schemes may be put to the test when the planned STEREO mission, carrying a coronagraph to an oblique viewpoint with respect to the Earth-Sun line, is realized. Nevertheless, this study also illustrates the kinds of questions and ambiguities that will arise without other supporting diagnostics, together with a better model of the CME-ICME connection.

**Acknowledgments.** We are thankful to N. Sheeley of NRL for his assistance with Solwind imagery and to R. Schwenn and K. Ivory of MPI for providing Helios-1 data. We also appreciate the useful information relevant to this paper contributed by J. Burkepile.

Hiroshi Matsumoto thanks K. Marubashi and another referee for their assistance in evaluating this paper.

## References

Burkepile, J. T., and O. C. St. Cyr., A revised and expanded catalogue of mass ejections observed by the Solar Maximum Mission coronograph, *Tech. Note NCAR/TN369 + STR* High Altitude Obs., Natl. Cent. for Atmos. Res., Boulder, Colo., 1993.

Burlaga, L. F., Magnetic clouds and force free fields with constant alpha, *J. Geophys. Res., 93*, 7917-7224, 1988.

Burlaga, L. F., Magnetic clouds, in *Physics of the Inner Heliosphere II*, edited by R. Schwenn and E. Marsch, 21, pp. 1-22, Springer-Verlag, New York, 1991.

Burlaga, L. F., E. Sittler, F. Mariani, and R. Schwenn, Magnetic loop behind an interplanetary shock: Voyager, Helios, and IMP 8 observations, *J. Geophys. Res., 86*, 6673-6684, 1981.

Burlaga, L. F., L. Klein, N. R. Sheeley Jr., D. J. Michel, R. A. Koomen, R. Schwenn, and H. Rosenbauer, A magnetic cloud and a coronal mass ejection, *Geophys. Res. Lett., 9*, 1317-1320, 1982.

Burlaga, L. F., K. W. Behannon, and L. W. Klein, Compound streams, magnetic clouds and major geomagnetic storms, *J. Geophys. Res., 92*, 5725-5734, 1987.

Cane, H. V., The evolution of interplanetary shocks, *J. Geophys. Res., 90*, 191-197, 1985.

Cargill, P. J., J. Chen, D. S. Spicer, and S. T Zalesak, Geometry of interplanetary magnetic clouds, *Geophys. Res. Lett., 22*, 647-650, 1995.

Chen, J., and D. A. Garren, Interplanetary magnetic clouds: Topology and driving mechanism, *Geophys. Res. Lett., 20*, 2319-2322, 1993.

Colin, L., The Pioneer Venus program, *J. Geophys. Res., 85*, 7575-7598, 1980.

Farrugia, C. J., V. A. Osherovich, and L. F. Burlaga, Magnetic flux rope versus the spheromak as models for interplanetary magnetic clouds. *J. Geophys. Res. 100*, 12993-12306, 1995.

Feynman, J., and S. F. Martin, The initiation of coronal mass ejections by newly emerging magnetic flux, *J. Geophys. Res., 100*, 3355-3367, 1995.

Gonzalez, W. D., J. A. Joselyn, Y. Kamide, H. Kroehl, G. Rostoker, B. Tsurutani, and V. Vasyliunas, What is a geomagnetic storm?, *J. Geophys. Res., 99*, 5771-5792, 1994.

Gonzalez, W. D., A. L. Chua de Gonzalez, A. Dal Lago, B. T. Tsurutani, J. K. Arballo, G. K. Lakhina, B. Buti, C. M. Ho, and S. T. Wu, Magnetic cloud field intensities and solar wind velocities, *Geophys. Res. Lett., 25*, 963-966, 1998.

Gosling, J. T., and D. J. McComas, Field line draping about fast coronal mass ejecta: A source of strong out-of-the-ecliptic interplanetary magnetic fields, *Geophys. Res. Lett., 14*, 355-358, 1987.

Gosling, J. T., E. Hildner, R. M. MacQueen, R. H. Munro, A. I. Poland, and C. L. Ross, The speeds of coronal mass ejection events, *Sol. Phys., 48*, 389-397, 1976.

Gosling, J. T., J. R. Asbridge, S. J. Bame, W. C. Feldman, and R. D. Zwickl, Observations of large fluxes of $He^+$ in the solar wind following an interplanetary shock, *J. Geophys. Res., 85*, 3431-3434, 1980.

Gosling, J. T., M. F. Thomsen, S. J. Bame, and R. Zwickl, The eastward deflection of fast coronal mass ejecta in interplanetary space, *J. Geophys. Res., 92*, 12399-12406, 1987a.

Gosling, J. T., D. N. Baker, S. J. Bame, W. C. Feldman, and R. D. Zwickl,

Bidirectional solar wind electron heat flux events, *J. Geophys. Res.*, *92*, 8519-8535, 1987b.

Gosling, J. T., D. J. McComas, J. L. Phillips, and S. J. Bame, Geomagnetic activity associated with Earth passage of interplanetary shock disturbances and coronal mass ejections, *J. Geophys. Res.*, *96*, 7831-7839, 1991.

Gosling, J. T., D. J. McComas, J. L. Phillips, and S. J. Bame, Counterstreaming solar wind halo electron events: Solar cycle variations, *J. Geophys. Res.*, *97*, 6531-6535, 1992.

Gosling, J. T., D. J. McComas, J. L. Phillips, L. A. Weiss, V. J. Pizzo, B. E. Goldstein, and R. J. Forsythe, A new class of forward-reverse shock pairs in the solar wind, *Geophys. Res. Lett.*, *21*, 2271-2274, 1994.

Hirshberg, J., Y. Nakagawa, and R. E. Wellck, Propagation of sudden disturbances through nonhomogeneous solar wind, *J. Geophys. Res.*, *79*, 3726-3730, 1974.

Hoeksema, J. T., and X. Zhao, Prediction of magnetic orientation in driver gas associated-Bz events, *J. Geophys. Res.*, *97*, 3151-3157, 1992.

Howard, R., N. R. Sheeley, M. J. Koomen, and D. J Michels, Coronal mass ejections: 1979-1981, *J. Geophys. Res.*, *90*, 8173-8191, 1985.

Hundhausen, A. J., J. T. Burkepile, and O.C.St. Cyr., Speeds of coronal mass ejections: SMM observations from 1980 and 1984-1989, *J. Geophys. Res.*, *99*, 6543-6552, 1994.

Intriligator, D. S., J. H. Wolfe, and J. D. Mihalov, The Pioneer Venus Orbiter plasma analyzer experiment, *IEEE Trans. Geosci. Remote Sens.*, *18*, 39-42, 1980.

Kahler, S. W., Coronal mass ejections and long rise times of solar energetic particle events, *J. Geophys. Res.*, *98*, 5607-5615, 1993.

Klein, L. W., and L. F. Burlaga, Interplanetary magnetic clouds at 1 AU, *J. Geophys. Res.*, *87*, 613-624, 1982.

Koomen. M. J., C. R. Detwiler, G. E. Bruckner, H. W. Cooper, and R. Tousey, White light coronagraph in OS0-7, *App. Opt.*, *14*, 743-751, 1975.

Lindsay, G. M., J. G. Luhmann, C. T. Russell, and P. R. Gazis, On the sources of interplanetary shocks at 0.72 AU, *J. Geophys. Res.*, *99*, 11-17, 1994.

Low, B. C., Equilibrium and dynamics of coronal magnetic fields, *Annu. Rev. Astron. Astrophys.*, *28*, 491-524, 1990.

Mariani, F., N. F. Ness, L. F. Burlaga, B. Bavassano, and U. Villante, The large-scale structure of the interplanetary magnetic field between 1 and 0.3 AU during the primary mission of Helios 1, *J. Geophys. Res.*, *83*, 5161-5166, 1978.

Marubashi, K., Structure of the interplanetary magnetic clouds and their solar origins, *Adv. Space Res.*, *6*, 335-338, 1986.

MacQueen, R. M., A. Csoeke-Poeckh, E. Hildner, L. House, R. Reynolds, A. Stranger, H. Tepoel and W. Wagner, The high altitude coronograph/polarimeter on the Solar Maximum Mission, *Sol. Phys.*, *65*, 91-109, 1980.

Michels, D. J., R. A. Howard, M. J. Koomen, and N. R. Sheeley Jr., Satellite observations of the outer corona near sunspot maximum, in *Radio Physics of the Sun*, edited by M. R. Kundu and T. E. Gergeley, *Symp. Int. Astron. Union*, *86*, 439-442, 1980.

Mihalov, J. D., Distant heliospheric results on interplanetary shock propagation, *J. Geophys. Res. 90*, 209-215, 1985.

Munro, R. H., J. T. Gosling, E. Hildner, R. M. MacQueen, A. I. Poland, and C. L. Ross, The association of coronal mass ejection transients with other forms of solar activity, *Sol. Phys.*, *61*, 201-215, 1979.

Richardson, I. G., C. J. Farrugia, and D. Winterhalter, Solar activity and coronal mass ejections on the western hemisphere of the Sun in mid-August 1989: Association with interplanetary observations at the ICE and IMP 8 spacecraft, *J. Geophys. Res.*, *99*, 2513-2529, 1994.

Russell, C. T., R. C. Snare, J. D. Means, and R.C. Elphic, Pioneer-Venus Orbiter fluxgate magnetometer, *IEEE Trans. Geosci. Remote Sens.*, *18*, 32-35, 1980.

Schwenn, R., Direct correlation between coronal transient and interplanetary disturbances, *Sp. Sci. Rev.*, *34*, 85-99, 1983.

Sheeley, N. R., Jr., D. J. Michels, R. A. Howard, and M. J. Koomen, Initial observations with the Solwind coronagraph, *Astron. Lett.*, *237*, 99-101, 1980.

Sheeley, N. R., R. A. Howard, M. J. Koomen, D. J. Michels, R. Schwenn, K. H. Muhlhauser, and H. Rosenbauer, Coronal mass ejections and interplanetary shocks, *J. Geophys. Res.*, *90*, 163-175, 1985.

Sheeley, N. R., Jr., et al., Measurements of flow speeds in the corona between 2 and 30 Rs, *Astrophys. J.*, *484*, 472-478, 1997.

Tang, F., B. T. Tsurutani, W. D. Gonzales, S. I. Akasofu., and E. J. Smith, Solar sources of interplanetary southward Bz events responsible for major magnetic storms (1978-1979), *J. Geophys. Res.*, *94*, 3535-3541, 1989.

Tsurutani, B. T., B. E. Goldstein, E. J. Smith, W. D., Gonzales, F. Tang, S. I. Akasofu, and R. R. Anderson, The interplanetary and solar causes of geomagnetic activity, *Planet. Space Sci.*, *38*, 109-126, 1990.

Webb, D. F., The solar cycle variation of the rates of CME's and related activity, *Adv. Space Res.*, *11*(1), 37-40, 1991.

---

J. T. Gosling, Los Alamos National Laboratory, Los Alamos, NM 87545.

G. M. Lindsay, HQ AFSPC/DRFS, Peterson AFB, Colorado Springs, CO 80914.

J. G. Luhmann, Space Sciences Laboratory, University of California, Berkeley, CA 90745.

C. T. Russell, IGPP, University of California, Los Angeles, CA 90095. (ctrussell@igpp.ucla.edu).

(Received June 24, 1998; revised October 8, 1998;
Accepted January 26, 1999.)